Water Research 103 (2016) 205–214

Contents lists available at ScienceDirect

Water Research

journal homepage: www.elsevier.com/locate/watres

Identification of biotransformation products of citalopram formed in activated sludge

Vasiliki G. Beretsou [a], Aikaterini K. Psoma [a], Pablo Gago-Ferrero [a], Reza Aalizadeh [a], Kathrin Fenner [b, c], Nikolaos S. Thomaidis [a, *]

[a] Laboratory of Analytical Chemistry, Department of Chemistry, National and Kapodistrian University of Athens, Panepistimiopolis Zografou, 15771, Athens, Greece
[b] Eawag, Swiss Federal Institute of Aquatic Science and Technology, 8600, Dübendorf, Switzerland
[c] Department of Environmental Systems Science (D-USYS), ETH Zürich, 8092, Zürich, Switzerland

ARTICLE INFO

Article history:
Received 27 March 2016
Received in revised form
26 June 2016
Accepted 12 July 2016
Available online 14 July 2016

Keywords:
Citalopram
Metabolites
Transformation products
Retrospective analysis
LC-QTOF-MS
HILIC

ABSTRACT

Citalopram (CTR) is a worldwide highly consumed antidepressant which has demonstrated incomplete removal by conventional wastewater treatment. Despite its global ubiquitous presence in different environmental compartments, little is known about its behaviour and transformation processes during wastewater treatment. The present study aims to expand the knowledge on fate and transformation of CTR during the biological treatment process. For this purpose, batch reactors were set up to assess biotic, abiotic and sorption losses of this compound. One of the main objectives of the study was the identification of the formed transformation products (TPs) by applying suspect and non-target strategies based on liquid chromatography quadrupole-time-of-flight mass spectrometry (LC-QTOF-MS). The complementary use of reversed phase liquid chromatography (RPLC) and hydrophilic interaction liquid chromatography (HILIC) for the identification of polar TPs, and the application of in-house developed quantitative structure-retention relationship (QSRR) prediction models, in addition to the comprehensive evaluation of the obtained MS/MS spectra, provided valuable information to support identification. In total, fourteen TPs were detected and thirteen of them were tentatively identified. Four compounds were confirmed (*N*-desmethylCTR, CTR amide, CTR carboxylic acid and 3-oxo-CTR) through the purchase of the corresponding reference standard. Probable structures based on diagnostic evidence were proposed for the additional nine TPs. Eleven TPs are reported for the first time. A transformation pathway for the biotransformation of CTR was proposed. The presence of the identified TPs was assessed in real wastewater samples through retrospective analysis, resulting in the detection of five compounds. Finally, the potential ecotoxicological risk posed by CTR and its TPs to different trophic levels of aquatic organisms was evaluated by means of risk quotients.

1. Introduction

Citalopram (CTR), a selective serotonin re-uptake inhibitor (SSRI), is a compound of interest due to its worldwide high consumption for the treatment of depression. Following oral ingestion, it undergoes hepatic metabolism in order to form more hydrophilic excretable compounds. The phase I human metabolites of CTR include *N*-desmethylCTR, *N*-didesmethylCTR, CTR-*N*-oxide, and a CTR propionic acid derivative (Kosjek and Heath, 2010; Silva et al., 2012). Several studies carried out in different countries reported the presence of CTR in different environmental matrices, including influent wastewaters (IWW), effluent wastewaters (EWW), sewage sludge, surface waters and biota (Silva et al., 2012, 2015). A literature review of worldwide levels in different environmental compartments (Table S1, Section S1) reveals CTR's global ambiguous distribution. However, fewer studies (Table S2, Section S1) have focused on the presence of CTR's metabolites in environmental samples: *N*-desmethylCTR has been detected in IWW, EWW, sewage sludge (Schlusener et al., 2015; Subedi and Kannan, 2015), surface waters (Schlusener et al., 2015) and biota (Metcalfe et al., 2010), while *N*-didesmethyl CTR was only detected in one study in IWW and EWW samples (Vasskog et al., 2008).

* Corresponding author.
E-mail address: ntho@chem.uoa.gr (N.S. Thomaidis).

http://dx.doi.org/10.1016/j.watres.2016.07.029
0043-1354/

In contrast to the large number of studies evaluating the occurrence of CTR, the studies dealing with its fate and transformation processes in the environment or during wastewater treatment are scarce. For CTR, biodegradation is considered to be the most important removal mechanism during wastewater treatment while the contribution of sorption and volatilization seems to be insignificant (Alvarino et al., 2015; Hörsing et al., 2011, 2012). The compound was moderately biodegraded under both aerobic and anoxic conditions with an approximate elimination rate of 60% and 40%, respectively, in the studies carried out by Suarez et al. (Suarez et al., 2010, 2012). Moreover, CTR was found to be hydrolytically stable at pH 5, 7 and 9, whereas photodegradation at pH 9 resulted in the formation of two photoproducts: *N*-desmethylCTR and CTR-*N*-oxide, both tentatively identified by LC-MS/MS (Kwon and Armbrust, 2005). Another study, dealing with its fate during water treatment with O_3 and ClO_2 oxidation, reported *N*-desmethylCTR, CTR-*N*-oxide and three other TPs (3-oxo-CTR, a hydroxylated dimethylamino-side chain derivative and a defluorinated derivative of CTR) (Hörsing et al., 2012).

Apart from the presence and the fate of CTR and its TPs in the environment, another aspect to assess is their toxicity by determining possible effects that can be expected at relevant concentrations. CTR has been found to present low acute and chronic toxicity so far, being considered the least toxic among the SSRIs, but also the one least tested for ecotoxicological effects (Christensen et al., 2007; Silva et al., 2015).

Therefore, the detection and identification of biotransformation TPs is a necessary but challenging task, which requires the use of modern high resolution mass spectrometric (HR-MS) systems and appropriate analytical strategies (Bletsou et al., 2015; Picó and Barceló, 2015). In this regard, hydrophilic interaction liquid chromatography (HILIC) is becoming an attractive alternative (or complement) to the commonly used reversed phase liquid chromatography (RPLC), due to its ability to separate hydrophilic compounds which are poorly retained on RPLC columns (Zonja et al., 2014; Gago-Ferrero et al., 2015). The use of reliable quantitative structure-retention relationships (QSRR) prediction models is also a very useful tool for the identification of suspect and unknown compounds (Gago-Ferrero et al., 2015; Aalizadeh et al., in press).

The present study aims to contribute to the existing knowledge on fate and transformation of CTR during the biological treatment process. For this purpose, biodegradation batch experiments under aerobic conditions were carried out to investigate its behaviour and the formation of TPs during activated sludge treatment. The identification of the formed TPs was based on an integrated LC-HRMS-based workflow, using both suspect and non-target approaches. Analysis was performed by both RPLC and HILIC to investigate their complementarity for the detection of additional compounds. In-house developed QSRR prediction models were also used to support identification. The presence of the identified TPs in the batch experiments was investigated in real wastewater samples from the WWTP of Athens through retrospective analysis. Finally, an environmental risk assessment study was performed by using the predictive ECOSAR model to assess the potential threat for aquatic organisms.

2. Materials and methods

2.1. Chemicals and reagents

Details on the used chemicals and reagents are provided in the Supplementary material (Section S2).

2.2. Sampling

Activated sludge and EWW were sampled from the WWTP of Athens (Greece) for the biotransformation batch experiments. Moreover, 24-h composite flow-proportional samples of IWW and EWW, collected in March of 2014 and 2015 during eight consecutive days for each year, were used for the retrospective analysis of CTR TPs.

The WWTP of Athens is designed with primary sedimentation, activated sludge process with biological nitrogen (nitrification, denitrification) and phosphorus removal and secondary sedimentation. The hydraulic retention time in bioreactors was 9 h, the sludge retention time was 7 days and the estimated sewage flow for the collected samples was 750,000 m^3 day^{-1}. The residential population connected to the WWTP was 3,700,000. The WWTP is designed to serve a population equivalent of 5,200,000 and thus is by far the largest in Greece. A schematic flow diagram of the wastewater treatment in WWTP of Athens is presented in Supplementary material (Fig. S1, Section S3) along with the sampling points for IWW, EWW and activated sludge.

The suspended solid (SS) content of the activated sludge was 3.7 g L^{-1} and its volatile solid content was 3.0 g L^{-1} during the sampling period. The main average qualitative characteristics of the EWW samples used during the experimental period were: pH = 7.4; COD = 34 mg L^{-1}; BOD = 9.1 mg L^{-1}; TSS = 8 mg L^{-1}; NH_4-N = 0.67 mg L^{-1}; NO_3-N = 7.22 mg L^{-1}; P_{total} = 1.6 mg L^{-1}.

Activated sludge, IWW and EWW were collected in pre-cleaned, high-density polyethylene (HDPE) bottles. Biotransformation experiments commenced within 24 h after sampling. Wastewater samples were filtered through sterile glass fiber filters (GFFs) of pore size 0.7 μm immediately upon arrival at the laboratory, then stored in the dark at 4 °C until analysis within the next 24 h.

2.3. Biotransformation batch experiments

Biotransformation of CTR was investigated within a 6-day batch experiment. The biodegradation test system was prepared in 500 mL amber glass bottles with 200 mL of appropriate content.

Activated sludge was sampled directly from the aeration tank (Supplementary material, Section S3, Fig. S1) in order to seed the biotic reactor. Total suspended solids (TSS) concentration was measured using Standard Method 2540B (Clesceri et al., 1998). Additionally, two different control experiments were carried out. A batch reactor with EWW was run as hydrolysis and volatilization control (abiotic reactor) and another batch reactor with sterilized sludge (autoclaved at 121 °C for 24 h) diluted with EWW was set up to examine the sorption losses (sorption reactor) (Gulde et al., 2014). All bioreactors were spiked with 400 μL of CTR standard stock solution to obtain a final concentration of 2 mg L^{-1}. A non-spiked blank reactor seeded with activated sludge was always run in parallel to check for potential cross-contamination between sampling and to subtract the background caused by the natural sludge matrices in post-acquisition data treatment.

Each bioreactor was loosely covered with a perforated cap to allow oxygen diffusion, but avoiding contamination and evaporation, and placed on a magnetic stirrer to further simulate the conventional activated sludge system. Initial pH was in the range 7.4–8.4 and the bottles were at controlled temperature (20 °C) under dark conditions.

Samples were taken immediately after spiking, 1, 2, 4, 6, 8 and 10 h later and after 1, 2, 3, 4, 5 and 6 days. 1 mL was sampled from each reactor, filtered first through a 1.0 μm disposable GF syringe filter and then through a 0.2 μm regenerated cellulose (RC) syringe filter and divided in two aliquots. In RPLC mode, the filtrates were diluted with MeOH to achieve an in-vial composition of 50:50

MeOH:H_2O. For HILIC analysis, the filtrates were dried under a gentle stream of nitrogen and reconstituted in ACN:H_2O (95:5) prior to analysis.

Analysis was carried out using an ultrahigh-performance liquid chromatography (UHPLC) (Dionex UltiMate 3000 RSLC, Thermo Fisher Scientific, Dreieich, Germany) interfaced to a Quadrupole-Time of Flight mass spectrometer (QTOF Maxis Impact, Bruker Daltonics, Bremen, Germany) in both RPLC and HILIC modes. Instrumental analysis is described extensively in the Supplementary material (Section S4).

2.4. Analysis of WWTP samples

IWW and EWW samples were extracted using a slightly modified protocol from the one developed by Kern et al. (Kern et al., 2009). Analysis was carried out using the UHPLC-QTOF-MS system in RPLC mode. Detailed information about instrumental analysis and sample preparation are given in the Supplementary material (Sections S4 and S5).

2.5. Suspect and non-target screening for the identification of TPs

A two-step post-acquisition data processing approach was employed to detect and identify candidate TPs of CTR (Gago-Ferrero et al., 2015).

As a first step, a suspect database of plausible TPs was compiled by using two different *in silico* prediction tools: (1) the Eawag-Biocatalysis/Biodegradation Database Pathway Prediction System (Eawag-BBD/PPS) (http://eawag-bbd.ethz.ch/predict/), an artificial intelligence system, which predicts microbial metabolic reactions based on biotransformation rules set in the Eawag-BBD and scientific literature. Eawag PPS was used with the "relative reasoning mode" switched off, and (2) the MetabolitePredict software (Metabolite Tools 2.0, Bruker Daltonics, Bremen, Germany), a rule-based expert system, which predicts metabolites from Phase I, II and Cytochrome P450 reactions. The prediction results from both programs included the molecular formula as well as the structures of the generated TPs from two subsequent reactions in the metabolic pathway. Already known and reported metabolites from the literature were also added to the suspect database (Kosjek and Heath, 2010; Silva et al., 2012).

All samples taken at different sampling times (time interval samples) were screened in full scan, in both chromatographic systems and in both ionization modes, for the detection of suspect TPs from the database. The criteria used for the reduction of features in both chromatographic modes included a threshold in peak area ($\geq$2000 for ESI(+) and $\geq$800 for ESI(−)), a threshold in intensity counts ($\geq$500 for ESI(+) and $\geq$200 for ESI(−)), a threshold in mass accuracy of ±5 ppm on the monoisotopic peaks, the existence of a good isotopic pattern fit ($\leq$100 mSigma) and the chromatographic retention time plausibility in RPLC and HILIC, using in-house QSRR prediction models (Aalizadeh et al., in press; Aalizadeh and Thomaidis, 2015). Additional criteria for the identification of the suspects were the existence of a meaningful time trend during the batch experiments, their absence (or presence at very low levels) in the zero-time samples, the blank and the control samples.

As a second step, samples were also screened for additional TPs not present in the suspect database, following a non-target approach. Background subtraction and peak picking were carried out using Metabolite Detect (Metabolite Tools 2.0, Bruker Daltonics, Bremen, Germany) in order to find TPs present in the biotic samples, but absent in the control samples, and that showed a meaningful time trend. Chromatograms of the biotic samples were compared with those of the control samples, using the following parameters in Metabolite Detect software: subtraction algorithm eXpose mode, delta time $\leq$0.1 min, delta mass $\leq$0.05 m/z and ratio 5.

Structure elucidation of both suspect and non-target TPs was based on the use of characteristic fragmentation (i.e., fragmentation pattern) during data-dependent MS/MS fragmentation events. The fragmentation pattern of the parent compound and TPs with available reference standards (*N*-desmethylCTR, CTR amide, CTR carboxylic acid, 3-oxo-CTR) was investigated and different diagnostic neutral losses as well the absence of characteristic fragment ions were recorded. Subsequently, the MS/MS spectrum of each detected TP was examined for the presence or absence of these diagnostic neutral losses or the presence of new ones, generalizing the previous "known" fragmentation pathways of CTR and its TPs in order to propose a new tentative structure.

The level of confidence for the identification of the detected compounds was determined according to Schymanski et al. (2014), where level 1 corresponds to confirmed structures (reference standard is available), level 2a to probable structures by library spectrum match, level 2b to probable structures by diagnostic evidence, level 3 to tentative candidate(s), level 4 to unequivocal molecular formulas, and level 5 to exact mass(es) of interest.

2.6. Retrospective suspect screening of CTR and its TPs

A retrospective suspect screening was performed in order to evaluate the occurrence of the identified TPs in real wastewater samples. The criteria for the tentative identification (or confirmation, when standards were available) of these TPs were the mass accuracy of the precursor ion ($\leq$5 ppm), isotopic fit (mSigma $\leq$100), identical chromatographic retention time (±0.2 min) and the presence of, at least, two qualifier ions in the MS/MS spectra.

2.7. Environmental risk assessment

Acute toxicity data were estimated by using the predictive ECOSAR (US EPA) model for three different trophic levels (fish, *daphnia magna* and algae) to evaluate the potential risk of CTR and its TPs, individually, in the aquatic environment. The ECOSAR program predicts toxicity by assessing the structural similarity of a given compound with compounds whose toxicity to aquatic organisms has already been experimentally determined (Thomaidi et al., 2015).

According to the Technical Guidance Document of the European Commission (European Commission (EC), 2003), the risk quotient (RQ) was calculated as the maximum Measured Environmental Concentration (MEC) divided by the Predicted No Effect Concentration (PNEC), which was calculated as the EC_{50} or LC_{50} value divided by 1000 for the case of acute toxicity data. MECs for the TPs are very rough estimates, based on the assumption that the parent compound and the TPs have the same response factor between peak area and concentration. For CTR, EC_{50} values for *daphnia magna* and algae were obtained from the literature (Christensen et al., 2007). RQs greater than 1 were considered indicative of an ecotoxicological risk for the aquatic environment.

3. Results and discussion

3.1. Degradation of CTR in batch experiments with activated sludge

Incomplete aerobic degradation of CTR was observed in the activated sludge system (biotic reactor) after 6 days. The concentration of CTR (spiked at 2 mg L^{-1}) exponentially decreased by approximately 70% during the first 3 days and then remained stable over the next 3 days (Fig. S2a, Section S6). After 9 h (HRT of WWTP),

approximately 40% of CTR has been removed. Even prolongation of the experimental time up to 6 days did not result in full removal of the parent compound. These results are in agreement with literature indicating moderate removal of CTR during full-scale wastewater treatment (i.e., Spain 42% (Suarez et al., 2010); Portugal 16.5%–55.2% (Silva et al., 2014); Czech Republic up to 34% (Golovko et al., 2014); Canada 40%–32% (Lajeunesse et al., 2012) and 23% (Metcalfe et al., 2010); Norway 30%–48% (Vasskog et al., 2006) and 22%–55% (Vasskog et al., 2008)).

The control experiments with diluted autoclaved sludge (sorption reactor) showed that a fraction of 13% was lost due to sorption processes or reactions with sludge particles. These losses could also be explained by a partial reactivation of the autoclaved sludge as the sludge could be contaminated by active bacteria each time it was sampled (Huntscha et al., 2014). The control reactor with EWW (abiotic reactor) showed negligible losses (3%) of CTR as it was still present at the initial concentration after 6 days. Thus, decreasing CTR's concentration in the active bioreactor can be clearly associated with biological activity.

The pH was measured in the active bioreactor of the CTR degradation experiment and increased slightly from 7.35 to 8.15 within the first 48 h, and subsequently decreased continuously to pH 6.60 until CTR was removed by 70%. The decrease in pH is due to the release of protons during nitrification, which was an ongoing process in the biotic reactor. This trend was not observed for the abiotic and sorption control reactors, which did not contain active biomass and had an average pH of 8.5 ± 0.3 and 8.4 ± 0.3, respectively (Gulde et al., 2014).

3.2. Identification of biotransformation products of CTR

Parallel to the biodegradation of CTR under aerobic conditions, fourteen TPs were formed in the biotic reactor and identified through the use of the suspect and non-target screening approaches described in Section 2.5. All TPs were detected in the ESI(+) mode. Analysis performed in ESI(−) mode did not reveal any additional TPs. Thirteen out of the fourteen TPs were detected in both RPLC and HILIC systems while the remaining one (CTR 360B) was only detectable by HILIC. Comparison between the peak areas of CTR and the sum of peak areas of the detected TPs (based on the assumption that CTR and its TPs have the same response factor between peak area and concentration) suggested that some TPs may remained undetected (Fig. S2b, Section S6). However, to perform a complete mass balance, quantification of TPs with corresponding reference standards is required, which are currently unavailable for most of the TPs.

Fig. 1 shows the formation/elimination profile (Peak area *vs* time, from HILIC analyses) for all the detected TPs. CTR 311, CTR 339A, CTR 339B, CTR 341, CTR 343 and CTR 344 were the major TPs and were formed during the first 6 h of the experiment. The % formation of the major TPs, at the time point of their maximum formation, compared to the initial concentration of CTR were 14.6, 8.0, 5.6, 5.2, 2.8 and 1.5 for CTR341, CTR311, CTR339A, CTR343, CTR344 and CTR39B, respectively. The calculation was based on the assumption that the TPs and the parent compound have the same response factor. The other compounds were detected at lower intensity and their abundance increased after the first 24 h. CTR 341, CTR 359B and CTR 344 presented maximum peak intensities at 72, 96 and 120 h, respectively, and then started to decrease. All the other TPs continued to increase over the time course of the experiments.

It should be mentioned that four TPs (CTR 311, CTR 339A, CTR 341 and CTR 343) were also formed in the control reactors at very low abundances (Fig. S3, Section S7), probably catalyzed by matrix components (Wick et al., 2011). The formation of these compounds seems to be mainly a result of abiotic processes; the peak area of the formed TPs in control samples corresponded to maximally 5–10% of their peak area in biotic samples at 6 days.

The identification of the structure of the formed TPs was based on the comprehensive interpretation of the MS/MS spectra. Six important fragmentation patterns with diagnostic neutral losses were observed and are illustrated in Fig. 2. In all cases, the obtained spectra presented the neutral loss of a H_2O molecule directly from the precursor ion. *N*-oxides followed a different pattern with a direct cleavage of the $NH(CH_3)_2O$ group and a further elimination of H_2O. Subsequently, different diagnostic neutral losses occurred: the loss of NHCO (amides), CO_2 (carboxylic acids), NH_2CH_3 (*N*-desmethyls), CO (TPs with furan ring oxidized) and an additional H_2O molecule (hydroxylated TPs). TP identification of the individual TPs is discussed later in this Section.

Another important tool to support identification of TPs was the complementarity of RPLC and HILIC systems in order to obtain orthogonal confirmation, plus the detection of additional TPs. It is important to note that the identification of the CTR 360B was possible only in HILIC, since RPLC was not able to separate the isomers. Moreover, two in-house QSRR prediction models (Aalizadeh et al., in press; Aalizadeh and Thomaidis, 2015) were used as additional experimental evidence for the identification (Schymanski et al., 2014). Predicted retention times for most TPs in both chromatographic systems were in agreement with the experimental ones (Table S3, Section S8). The *N*-oxide derivatives (CTR 341, CTR 355, CTR 359B and CTR 360A) were rejected only by the HILIC QSRR model, since they were outside of its applicability domain. However, the proposed structures were strongly supported by the observed fragmentation pattern. More details about the acceptance window and confidence intervals for predicted retention times can be found in Section S8.

Table 1 summarizes the TPs with their corresponding theoretical monoisotopic mass of the precursor ions ($[M+H]^+$) and molecular formula, the time trend, the time of first appearance, the time corresponding to the maximum intensity, the reached identification levels and the proposed structures. The elemental composition of CTR and its TPs along with their main product ions used for their identification, the measured *m/z*, the theoretical *m/z* and the mass error in ppm in both RPLC and HILIC systems are summarized in Table S4 (Section S9). The XICs in RPLC and HILIC of the detected TPs at all the incubation time points (time trend) are shown in Figs. S5–S21 (Section S9). These figures also show the MS/MS spectra (obtained in RPLC and HILIC at the time point of maximum intensity) for each TP including the proposed structures for the fragments.

The obtained MS/MS spectrum of CTR along with its chromatograms in RPLC and HILIC are shown in Fig. S5. It can be observed that the ions *m/z* 307 ($C_{20}H_{20}FN_2^+$) and 280 ($C_{18}H_{15}FNO^+$) were formed by cleaving off a H_2O molecule and a dimethyl amino group ($NH(CH_3)_2$). The major characteristic fragment with *m/z* 262 ($C_{18}H_{13}FN^+$) can be explained by the cleavage of either a $NH(CH_3)_2$ unit from 307 or H_2O from 280. Further on, the fragment *m/z* 262 was subjected to losses of a methyl (CH_3) and an ethyl group (CH_2CH_2), exhibiting ions with *m/z* 247 ($C_{17}H_{10}FN^+$) and 234 ($C_{16}H_9FN^+$), respectively. Additional characteristic fragments of CTR were *m/z* 109 ($C_7H_6F^+$) and *m/z* 58 ($C_3H_8N^+$).

The structure assignment for the twelve TPs identified though suspect screening is presented below:

3.2.1. CTR 343 ($C_{20}H_{24}FN_2O_2^+$)

This TP has an additional atom of oxygen and two extra atoms of hydrogen in comparison to the parent compound. The MS/MS spectra (Fig. S6) showed diagnostic neutral losses of one H_2O molecule and a $NH(CH_3)_2$ group, producing the fragment *m/z* 280

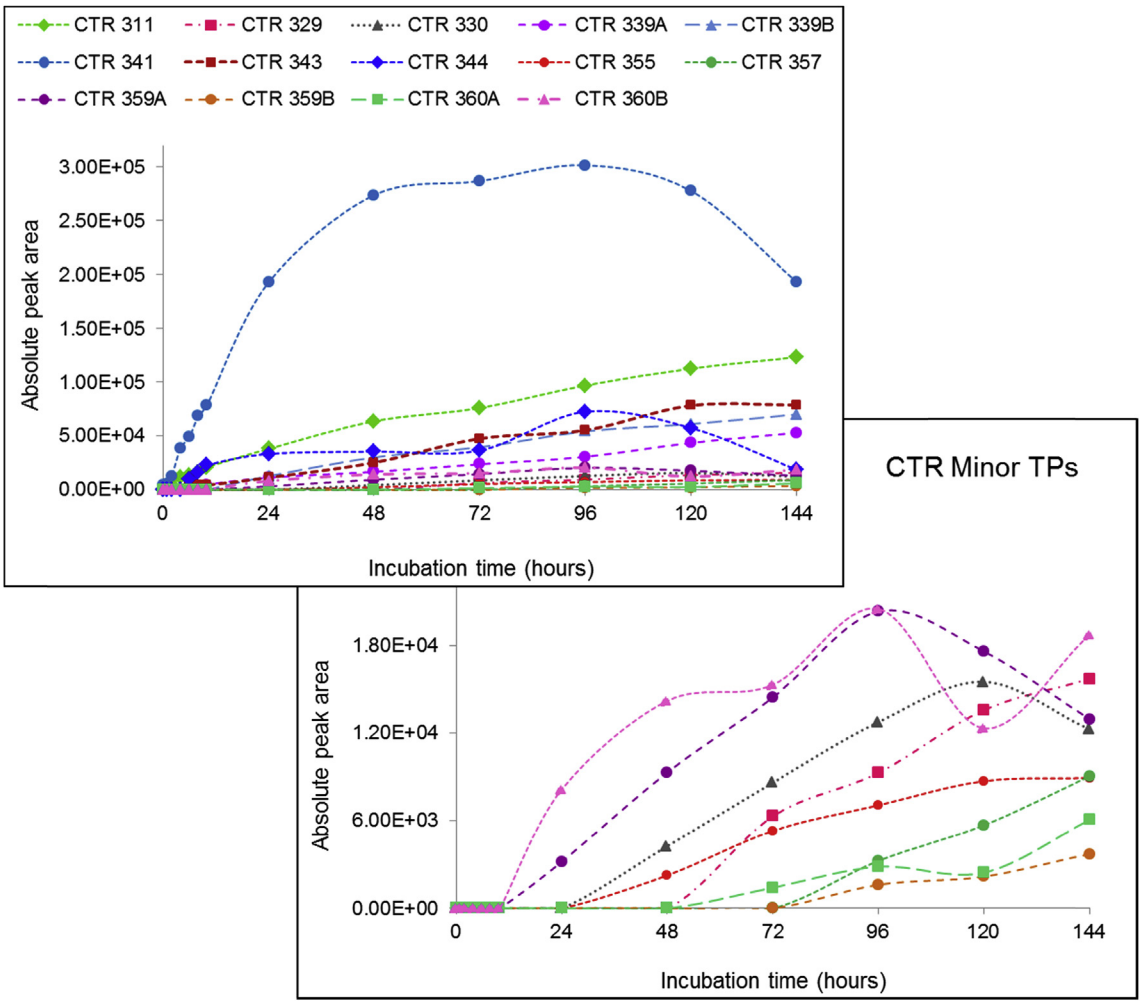

Fig. 1. Time profile of biotransformation products of CTR obtained by HILIC analysis.

($C_{18}H_{15}FNO^+$). A further loss of NHCO (indicating the presence of a primary amide moiety) formed the most abundant ion, *m/z* 237 ($C_{17}H_{14}F^+$), and a CTR amide structure was assigned. The identity of this compound was confirmed through the purchase of the corresponding standard, reaching identification level 1.

3.2.2. CTR 344 ($C_{20}H_{23}FNO_3^+$)

The elemental composition of this TP, along with the MS/MS spectra, indicated the presence of a carboxylic acid group (Fig. S7). Only one structure from the suspect database, CTR carboxylic acid, corresponds to the previous molecular formula. Likewise, a fragment ion with *m/z* 281 ($C_{18}H_{14}FO_2^+$) could be observed and the subsequent loss of CO_2 resulted in the formation of the major fragment *m/z* 237 ($C_{17}H_{14}F^+$). The standard of CTR carboxylic acid was purchased and the structure was confirmed, achieving identification level 1.

3.2.3. CTR 311 ($C_{19}H_{20}FN_2O^+$)

This compound lacks one carbon atom and two hydrogens in comparison to CTR, suggesting the loss of a methyl group. MS/MS spectra (Fig. S8) presented the subsequent eliminations of H_2O and NH_2CH_3 resulted in the formation of the ion *m/z* 262 ($C_{18}H_{13}FN_2^+$). The absence of the fragment *m/z* 58 ($C_3H_8N^+$) implied the transformation of the tertiary amino group into a secondary one. The identity of *N*-desmethylCTR was confirmed through the purchase and analysis of a reference standard. This compound is not only a TP that was formed during biodegradation experiments, but also a major metabolite of humans which is further metabolized into *N*-didesmethylCTR. However, the latter was not detected in the investigated treatment process, indicating that *N*-desmethylCTR was subjected to a transformation pathway that differs from human metabolism.

3.2.4. CTR 329 ($C_{19}H_{22}FN_2O_2^+$)

The fragment ions of this TP show similarities to those observed for CTR 343 and CTR 311 (Fig. S9). The loss of the NHCO group from the fragment *m/z* 280 that was formed through the elimination of H_2O and NH_2CH_3, resulting in the most abundant fragment (*m/z* 237 ($C_{17}H_{14}F^+$)), could be attributed to the presence of the amide group. Moreover, the absence of *m/z* 58 indicated the *N*-demethylated amide derivative. Thus, CTR 329 was proposed to be *N*-desmethylCTR amide, with an identification level 2b.

3.2.5. CTR 330 ($C_{19}H_{21}FNO_3^+$)

The MS/MS spectra of this TP (Fig. S10) showed the initial losses of H_2O and NH_2CH_3. Then, the abundant fragment ion *m/z* 237 ($C_{17}H_{14}F^+$) was formed by decarboxylation, in accordance with the carboxylic acids' fragmentation pattern. These evidences, along with the lack of the fragment *m/z* 58, suggested *N*-desmethylCTR carboxylic acid as the most plausible structure, with an identification level 2b.

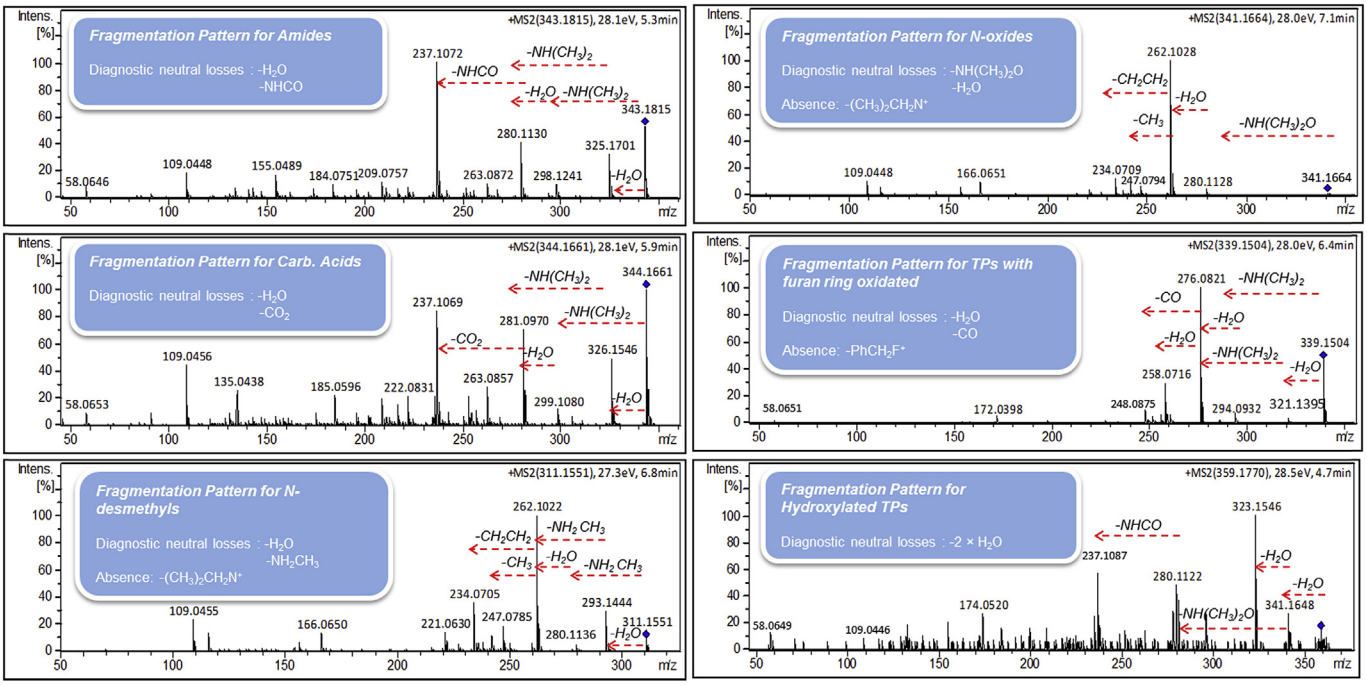

Fig. 2. Observed fragmentation patterns in selected MS/MS spectra of the formed TPs of CTR.

Table 1
Identified transformation products (TPs) of citalopram (CTR) during biodegradation batch experiments.

TP	Theoretical Monoisotopic Mass of $[M+H]^+$	Molecular formula	Time trend	First appearance (h)	Appearance of max. Intensity (h)	Identification level	Proposed structure
CTR 311	311.1554	$C_{19}H_{19}FN_2O$	↗	0	144	1	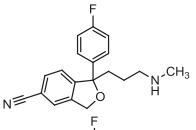
CTR 329	329.1660	$C_{19}H_{21}FN_2O_2$	↗	72	144	2b	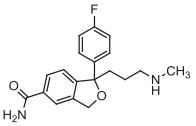
CTR 330	330.1500	$C_{19}H_{20}FNO_3$	↗	72	144	2b	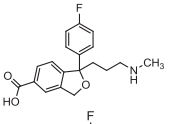
CTR 339A	339.1503	$C_{20}H_{19}FN_2O_2$	↗	4	144	2b	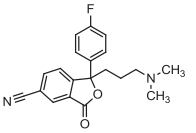
CTR 339B	339.1867	$C_{21}H_{23}FN_2O$	↗	6	144	4	–
CTR 341	341.1660	$C_{20}H_{21}FN_2O_2$	↗↘	2	72	2a	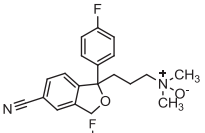
CTR 343	343.1816	$C_{20}H_{23}FN_2O_2$	↗	4	144	1	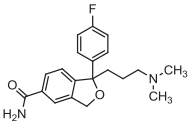

Table 1 (*continued*)

TP	Theoretical Monoisotopic Mass of $[M+H]^+$	Molecular formula	Time trend	First appearance (h)	Appearance of max. Intensity (h)	Identification level	Proposed structure
CTR 344	344.1656	$C_{20}H_{22}FNO_3$	↗↘	6	120	1	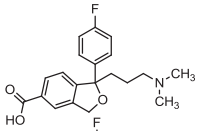
CTR 355	355.1452	$C_{20}H_{19}FN_2O_3$	↗	24	144	2b	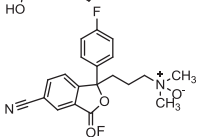
CTR 357	357.1609	$C_{20}H_{21}FN_2O_3$	↗	96	144	2b	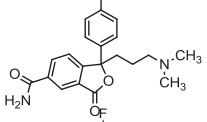
CTR 359A	359.1765	$C_{20}H_{23}FN_2O_3$	↗	72	144	3	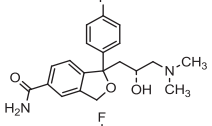
CTR 359B			↗↘	48	96	3	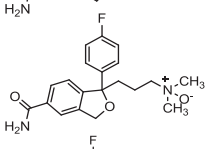
CTR 360A	360.1606	$C_{20}H_{22}FNO_4$	↗	–	144	2b	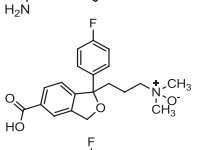
CTR 360B			↗	6	144	3	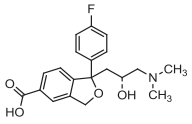

3.2.6. CTR 341 ($C_{20}H_{22}FN_2O_2^+$)

The elemental composition has an additional oxygen atom, in comparison to CTR and suggested a compound which could correspond to either an *N*-oxygenated or a hydroxylated TP according to the suspect list. The fragmentation pattern (Fig. S11) showed the direct cleavage of the $NH(CH_3)_2O$ group, forming the fragment ion *m/z* 280 ($C_{18}H_{15}FNO^+$), and the subsequent cleavage of H_2O forming *m/z* 262. Moreover, the absence of the characteristic fragment *m/z* 58 indicated the position of the additional oxygen, revealing that the structural change occurred in the tertiary amino group. Theoretically, the compound could be hydroxylated at the α-C position of the aliphatic chain, resulting in a hemiaminal which is rather unstable. Consequently, CTR 341 was proposed to be CTR-*N*-oxide, reaching an identification level 2a since the spectra were in agreement with available literature data (Hörsing et al., 2012). CTR-*N*-oxide is a human metabolite formed from CTR *via N*-oxidation. It was the most dominant compound in these experiments and peaked at 72 h after its appearance, indicating further transformation.

3.2.7. CTR 359A and CTR 359B ($C_{20}H_{24}FN_2O_3^+$)

Two TPs with the same elemental composition were eluted at t_R 4.7 and 5.6 min in RPLC system (Fig. S12). The differences in the MS/MS spectra proved their different identity. However, both MS/MS spectra showed similarities with the fragmentation pattern of amides, implying the presence of an amide moiety.

More specifically, the MS/MS spectra of CTR 359A (Fig. S13) exhibited fragment ions at *m/z* 341 ($C_{20}H_{22}FN_2O_2^+$) and *m/z* 323 ($C_{20}H_{20}FN_2O^+$), both generated by one or two cleavages of H_2O. The cleavage of $NH(CH_3)_2O$ from *m/z* 341 produced the fragment *m/z* 280 ($C_{18}H_{15}FNO^+$), which along with the presence of the fragment *m/z* 58 ($C_3H_8N^+$) indicated two possible positions for the hydroxylation. Thus, CTR 359A was identified as a hydroxylated derivative of CTR amide (α- or β-hydroxylation of the aliphatic chain; α-hydroxylation could result in a hemiaminal, which are usually unstable compounds), remaining at identification level 3.

The fragmentation pattern of the second-eluted TP (Fig. S14) showed a direct loss of $NH(CH_3)_2O$ at *m/z* 298 ($C_{18}H_{17}FNO_2^+$). Further on, the absence of *m/z* 58 ($C_3H_8N^+$) suggested the formation of an *N*-oxygenated amide derivative, in accordance with the *N*-oxides' fragmentation pattern. With these evidences, CTR 359B was proposed to be the amide of CTR-*N*-oxide with an assigned identification level 2b.

3.2.8. CTR 360A and CTR 360B ($C_{20}H_{23}FNO_4^+$)

Only one TP was detected with this elemental composition in RPLC mode. However, when HILIC analysis was performed, two different compounds with the same elemental composition were detected (Fig. S15). Both MS/MS spectra presented the characteristic fragmentation pattern of carboxylic acids (Figs. S16 and S17). CTR 360A spectra presented also the direct elimination of $NH(CH_3)_2O$ at *m/z* 299 ($C_{18}H_{16}FO_3^+$) which along with the absence of *m/z* 58 ($C_3H_8N^+$), implied the presence of an *N*-oxide group. So, CTR 360A was proposed to be the carboxylic acid of CTR-*N*-oxide (level 2b). The

MS/MS spectra of CTR 360B showed similarities with the fragmentation pattern of the hydroxylated compounds, with the cleavage of two H_2O molecules and further loss of $NH(CH_3)_2O$. Thus, CTR 360B was suggested to be a hydroxylated derivative of CTR carboxylic acid (α- or β-hydroxylation of the aliphatic chain; β-hydroxylation is more likely due to instability of hemiaminals) (level 3).

3.2.9. CTR 339A ($C_{20}H_{20}FN_2O_2^+$)

The elemental composition of this TP contains one additional oxygen atom and two hydrogen atoms less than the one corresponding to CTR. It can be observed (Fig. S18) that the crucial fragment ions at *m/z* 258 ($C_{18}H_9FN^+$) and *m/z* 248 ($C_{17}H_{11}FN^+$), associated with the elimination of H_2O and CO, respectively, indicated the oxidation of the furan ring and denoted the proposed structure of 3-oxo-CTR. It should be noticed that the fluorinated analogue with *m/z* 109 ($C_7H_6F^+$), which was a diagnostic fragment of CTR and its TPs, was absent here. A commercial standard of 3-oxo-CTR was purchased and the identity of the compound was confirmed *via* appropriate MS/MS and t_R matching, reaching finally identification level 1.

3.2.10. CTR 357 ($C_{20}H_{22}FN_2O_3^+$)

Although the suspect database included several double-hydroxylated substituted compounds, the fragmentation pattern of this TP (Fig. S19) did not correspond to any of them. The absence of the characteristic fragment *m/z* 109 was associated with oxidations in the furan ring as observed for CTR 339A, while the diagnostic loss of NHCO suggested the presence of an amide group. As a result, CTR 357 was proposed to be the oxidized derivative of CTR amide, allowing the assignment of an identification level 2b.

3.2.11. CTR 355

Apart from the compounds present in the suspect list, two additional TPs were detected and evaluated through non-target screening: An unequivocal molecular formula corresponding to $C_{20}H_{19}FN_2O_3$ was assigned to this TP, involving two additional oxygen atoms and two hydrogen atoms less in comparison to CTR. The MS/MS spectra (Fig. S20) displayed two distinct features: on one hand, the direct cleavage of $NH(CH_3)_2O$ along with the absence of *m/z* 58 provided strong evidence for the formation of an *N*-oxide moiety; on the other hand, the lack of the fragment *m/z* 109, together with the two H_2O losses, implied the formation of a 3-oxo-CTR derivative. Moreover, the conserved fragment ions at *m/z* 294 and 276 clearly indicated that the second oxidation occurred in the furan ring. Thus, CTR 355 was tentatively identified as a double-oxidized TP of CTR (level 2b).

3.2.12. CTR 339B

An unequivocal molecular formula corresponding to $C_{21}H_{23}FN_2O$ was annotated for this non-target TP. This elemental composition suggested the introduction of a methyl group in the initial structure. However, taking into account the MS/MS spectra (Fig. S21), it was not possible to go beyond the determination of the unequivocal molecular formula (level 4).

3.3. Proposed transformation pathway of CTR

A pathway for the biotic transformation of CTR, based on both the chemical structures of the identified TPs and the sequence of TP formation in the batch system, was proposed and is shown in Fig. 3. Oxidative reactions, such as hydroxylation, oxidation, *N*-oxidation and *N*-demethylation, were observed as the primary biotransformation mechanisms as well as nitrile hydrolysis and amide hydrolysis. All these processes were reported recently in a comprehensive study for amine-containing compounds (Gulde et al., 2016) and previously for amide-containing compounds (Helbling et al., 2010).

3.4. Retrospective analysis of CTR and its TPs in real wastewater samples

The occurrence of the identified TPs was assessed in real wastewater. To this end, a total of 32 samples from the WWTP of Athens (16 IWW and 16 EWW samples), previously analyzed by RPLC-QTOF-MS, were retrospectively screened without the need for additional injections of sample extracts.

The parent compound CTR along with its primary metabolite *N*-desmethylCTR (CTR 311) was found in all evaluated wastewater samples. 3-oxo-CTR (CTR 339A) was the second most frequently detected compound, as it was present in 26 out of 32 wastewater samples analyzed, including IWW and EWW. CTR-*N*-oxide (CTR 341) was also detected in all EWW and in 7 out of 16 the IWW. This fact can be easily explained since this compound is also a human metabolite. The intra-week concentration profiles of these three TPs were qualitatively consistent with the one corresponding to the parent compound in the EWW samples, as it can be observed in Figs. S22–S23 (Section S10). This TP/parent compound agreement in the daily or weekly concentration profile has been previously described by Gago-Ferrero et al. (2015) as a valid strategy to obtain extra confidence in the identification of TPs. The same weekly concentration profile was also observed for *N*-desmethylCTR and CTR in the evaluated IWW samples (the other two TPs were not detected so the trend could not be evaluated; this could be the result of the higher matrix effect of the influent extracts) (Figs. S24–S25, Section S10). Finally, the compounds CTR amide (CTR 343) and CTR carboxylic acid (CTR 344) were only found in 3 and 1 EWW samples, respectively, as a result of the biotransformation of CTR during the activated sludge process.

The presence of TPs of CTR in wastewater samples can be attributed to three sources: (1) the direct input from human excreted metabolites in IWW, (2) the biological activity of microorganisms in the sewage system and (3) the biotransformation of CTR and metabolites during wastewater treatment. The first two sources are responsible for the detection of CTR metabolites in the IWW, while the third one is responsible for the presence of biotransformation products in EWW. To assess the origin of CTR TPs, transformation ratios were calculated by dividing the peak area of each TP of CTR with the peak area of CTR, both for IWW and EWW samples of 2014 and 2015. It should be noted that CTR and its TPs might have different response factors in the detection system. These ratios were compared with those derived from pharmacokinetic studies for CTR excretion and metabolism (Table S5, Section S10). The ratios in urine presented higher uncertainty than the ratios in the IWW and EWW due to the multiple factors that affect the human metabolism of drugs (Zanger, 2012). According to Table S5, the ratios for *N*-desmethyl CTR were similar in urine, IWW and EWW samples, denoting that the concentrations detected in the samples are originated mainly from the input of human excretions. CTR-*N*-oxide ratios were slightly lower in the IWW samples than in urine and EWW. Especially, the ratios in EWW of 2014 were relatively elevated. Thus, the detected concentrations of CTR-*N*-oxide could be attributed to the biological activity during wastewater treatment. For the other three detected TPs, no pharmacokinetic data were available since they are not human metabolites and it is the first time that they are reported. The ratios of 3-oxo-CTR were the same in the IWW of both years and in the EWW of 2014, but presented a slight increase in the EWW of 2015, indicating the biotransformation of the parent compound either in the sewer system or during the wastewater treatment. CTR amide and CTR carboxylic acid were only detected in the EWW samples,

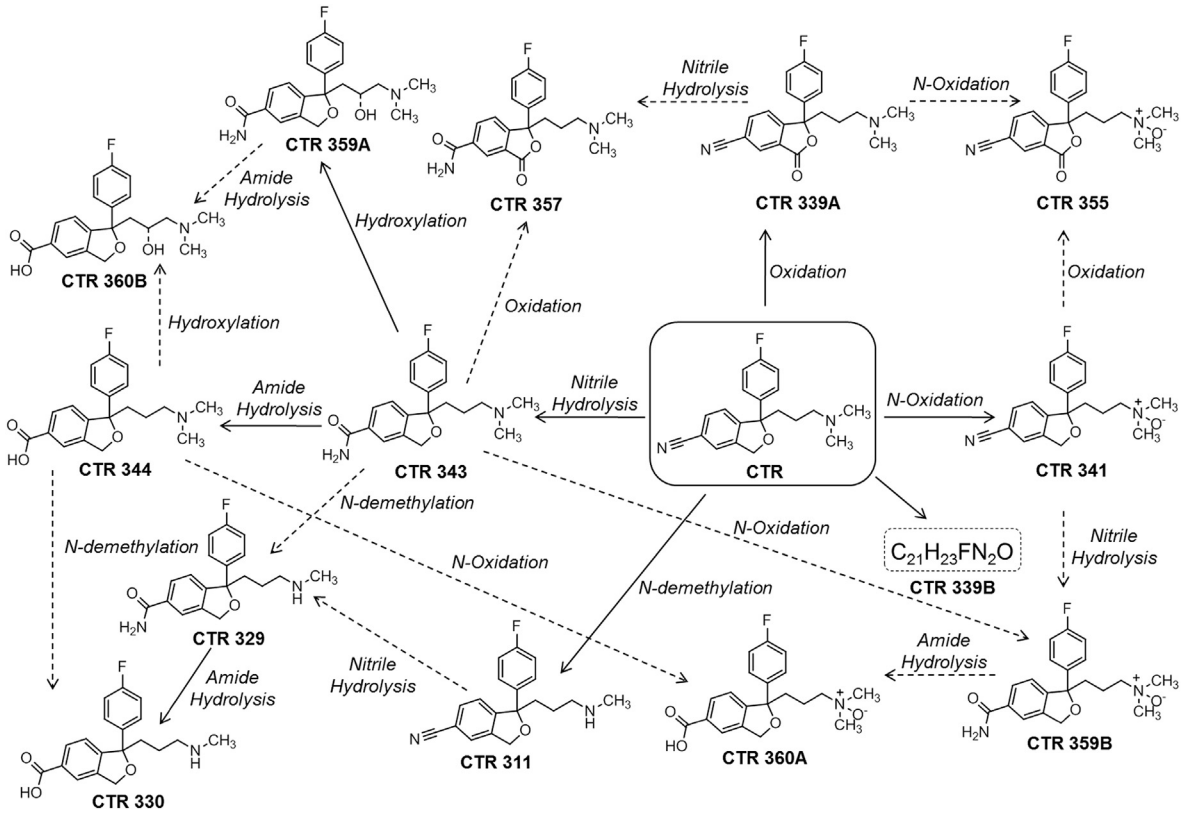

Fig. 3. Proposed biotransformation pathway for citalopram (CTR). Dotted arrows indicate that a single TP can be formed through different reactions from different precursors.

denoting that they are products of the biotransformation of CTR during the wastewater treatment. Finally, the excretion rate of *N*-didesmethylCTR was 0.15, thus its presence could be expected in the IWW, but it was not detected in any sample.

3.5. Environmental risk assessment of CTR and its confirmed TPs

Semi-quantitation of the identified TPs in the EWW sample collected on March 8, 2015 was performed in order to obtain the MEC values (Table S6, Section S11). MECs of the TPs were estimated from the response factor of CTR, based on the assumption that the parent compound and the TPs have the same response factor. This procedure could be fairly uncertain due to the fact that TPs and parent compounds might have different ionization efficiencies (Gulde et al., 2016). However, it was proved that the ionization efficiencies of 15 parent - TP pairs showed an average difference in ionization efficiency of 1.5, sufficient to yield a rough estimate of the MECs of TPs formed (Gulde et al., 2016). The concentrations of CTR and its TPs in the EWW sample, PNEC values and RQ estimated for each analyte are shown in Table S7, Section S11. It should be taken into account that the choice of data can obviously affect the outcome. According to these results, both CTR and its TPs have RQs lower than 1 and therefore no risk is expected from single compounds. However, given that a mixture of these compounds with the same pharmacological mechanisms exists in the environment, additive effects could be expected, making the real hazard potentially higher than calculated for the individual compounds (Christensen et al., 2007).

4. Conclusions

- The observed elimination rate (70%) for CTR in batch experiments with activated sludge can be associated with biological activity as control reactors showed insignificant removal of the parent compound.
- LC-QTOF-MS proved to be a powerful tool for the structure elucidation of the TPs; the orthogonal confirmation by RPLC and HILIC analysis, along with t_R prediction models, proved to be complementary strategies in the identification workflow. The importance of HILIC is emphasized in the detection of an additional TP (enabling the separation from its isomer), which could not be detected through RPLC analysis.
- In total, fourteen TPs were formed during the biodegradation experiments of CTR. Four out of them were confirmed with reference standards (*N*-desmethylCTR, CTR amide, CTR carboxylic acid and 3-oxo-CTR). A probable structure based on diagnostic evidence and tentative candidates were proposed for the additional seven and two TPs, respectively, while only one remained unidentified at identification level 4. *N*-desmethylCTR and CTR-*N*-oxide have been previously reported as human metabolites, whereas 3-oxo-CTR was an oxidative TP. To the authors' knowledge, this is the first study dealing with the identification of biotransformation TPs of CTR and eleven TPs are reported for the first time.
- Twelve TPs of CTR were identified through the use of suspect screening, and two additional TPs were detected by non-target screening. The performance of suspect screening (using *in silico* prediction software for the creation of the database) and non-target screening as independent and complementary approaches resulted in comprehensive identification of the formed TPs within specific biotransformation systems. Structure-based interpretation of the results was achieved for identification of preferences in biotransformation pathways of CTR.
- Two human metabolites (*N*-desmethylCTR and CTR-*N*-oxide) and three biotransformation TPs (3-oxo-CTR, CTR amide and CTR carboxylic acid) of CTR were detected in EWW samples

through retrospective suspect screening. It confirms that monitoring solely the presence of the parent compound CTR is not enough to assess the impact of this widely consumed pharmaceutical in the aquatic ecosystem.
- Risk quotients indicated no potential threat for the exposure of aquatic organisms regarding CTR and its TPs. However, available data regarding toxicity of CTR and its TPs in aquatic biota is very limited and further research is required on this aspect.

Acknowledgments

This project was implemented under the Greek Operational Program "Education and Lifelong Learning" and funded by the European Union (European Social Fund) and Greek National Resources (ARISTEIA 624, TREMEPOL project, http://tremepol.chem.uoa.gr/). Authors gratefully acknowledge the contribution of Dr. Rebekka Gulde for reviewing the manuscript, as well as Dr. Anna Bletsou and Nikiforos Alygizakis for the analysis of the WWTP samples.

Appendix A. Supplementary data

Supplementary data related to this article can be found at http://dx.doi.org/10.1016/j.watres.2016.07.029.

References

Aalizadeh, R., Thomaidis, N.S., Bletsou, A.A., Gago-Ferrero, P., 2016. QSRR models to support non-target high resolution mass spectrometric screening of emerging contaminants in environmental samples. J. Chem. Inf. Model. http://dx.doi.org/10.1021/acs.jcim.5b00752 (in press).

Aalizadeh, R., Thomaidis, N.S., 2015. Wide-scope QSRR models to support suspect and non-target screening of polar compounds in HILIC – ESI(+) – LC-HRMS. In: Proceedings of the 9th International Conference on Instrumental Methods of Analysis-modern Trends and Applications. Kalamata, Greece, 20–24 September 2015.

Alvarino, T., Suarez, S., Katsou, E., Vazquez-Padin, J., Lema, J.M., Omil, F., 2015. Removal of PPCPs from the sludge supernatant in a one stage nitritation/anammox process. Water Res. 68, 701–709.

Bletsou, A.A., Jeon, J., Hollender, J., Archontaki, E., Thomaidis, N.S., 2015. Targeted and non-targeted liquid chromatography-mass spectrometric workflows for identification of transformation products of emerging pollutants in the aquatic environment. Trends Anal. Chem. – Trac. 66, 32–44.

Christensen, M., Faaborg-Andersen, S., Ingerslev, F., Baun, A., 2007. Mixture and single-substance toxicity of selective serotonin reuptake inhibitors toward algae and crustaceans. Environ. Toxicol. Chem. 26, 85–91.

Clesceri, L.S., Greenberg, A.E., Eaton, A.D., 1998. Standard Methods for the Examination of Water and Wastewater, twentieth ed. American Public Health Association, American Water Works Association, Water Environment Federation, Baltimore, Maryland.

European Commission (EC), 2003. Technical Guidance Document in Support of Commission Directive 93/67/EEC on Risk Assessment for New Notified Substances, Commission Regulation (EC) No 1488/94 on Risk Assessment for Existing Substances, Directive 98/8/EC of the European Parliament and of the Council Concerning the Placing of Biocidal Products on the Market, Part II. Office for Official Publications of the European Communities, Luxembourg.

Gago-Ferrero, P., Schymanski, E.L., Bletsou, A.A., Aalizadeh, R., Hollender, J., Thomaidis, N.S., 2015. Extended suspect and non-target strategies to characterize emerging polar organic contaminants in raw wastewater with LC-HRMS/MS. Environ. Sci. Technol. 49 (20), 12333–12341.

Golovko, O., Kumar, V., Fedorova, G., Randak, T., Grabic, R., 2014. Seasonal changes in antibiotics, antidepressants/psychiatric drugs, antihistamines and lipid regulators in a wastewater treatment plant. Chemosphere 111, 418–426.

Gulde, R., Helbling, D.E., Scheidegger, A., Fenner, K., 2014. pH-dependent biotransformation of ionizable organic micropollutants in activated sludge. Environ. Sci. Technol. 48 (23), 13760–13768.

Gulde, R., Meier, U., Schymanski, E.L., Kohler, H.-P.E., Helbling, D.E., Derrer, S., Rentsch, D., Fenner, K., 2016. Systematic exploration of biotransformation reactions of amine-containing micropollutants in activated sludge. Environ. Sci. Technol. 50 (6), 2908–2920.

Helbling, D.E., Hollender, J., Kohler, H.-P.E., Fenner, K., 2010. Structure-based interpretation of biotransformation pathways of amide-containing compounds in sludge-seeded bioreactors. Environ. Sci. Technol. 44 (17), 6628–6635.

Hörsing, M., Ledin, A., Grabic, R., Fick, J., Tysklind, M., la Cour Jansen, J., Andersen, H.R., 2011. Determination of sorption of seventy-five pharmaceuticals in sewage sludge. Water Res. 45 (15), 4470–4482.

Hörsing, M., Kosjek, T., Andersen, H.R., Heath, E., Ledin, A., 2012. Fate of citalopram during water treatment with O_3, ClO_2, UV and Fenton oxidation. Chemosphere 89 (2), 129–135.

Huntscha, S., Hofstetter, T.B., Schymanski, E.L., Spahr, S., Hollender, J., 2014. Biotransformation of benzotriazoles: insights from transformation product identification and compound-specific isotope analysis. Environ. Sci. Technol. 48 (8), 4435–4443.

Kern, S., Fenner, K., Singer, H., Schwarzenbach, R.P., Hollender, J., 2009. Identification of transformation products of organic contaminants in natural waters by computer-aided prediction and high-resolution mass spectrometry. Environ. Sci. Technol. 43, 7039–7046.

Kosjek, T., Heath, E., 2010. Tools for evaluating selective serotonin re-uptake inhibitor residues as environmental contaminants. Trends Anal. Chem. – Trac. 29 (8), 832–847.

Kwon, J.-W., Armbrust, K.L., 2005. Degradation of citalopram by simulated sunlight. Environ. Toxicol. Chem. 24, 1618–1623.

Lajeunesse, A., Smyth, S.A., Barclay, K., Sauve, S., Gagnon, C., 2012. Distribution of antidepressant residues in wastewater and biosolids following different treatment processes by municipal wastewater treatment plants in Canada. Water Res. 46 (17), 5600–5612.

Metcalfe, C.D., Chu, S., Judt, C., Li, H., Oakes, K.D., Servos, M.R., Andrews, D.M., 2010. Antidepressants and their metabolites in municipal wastewater, and downstream exposure in an urban watershed. Environ. Toxicol. Chem. 29 (1), 79–89.

Picó, Y., Barceló, D., 2015. Transformation products of emerging contaminants in the environment and high-resolution mass spectrometry: a new horizon. Anal. Bioanal. Chem. 407, 6257–6273.

Schlusener, M.P., Hardenbicker, P., Nilson, E., Schulz, M., Viergutz, C., Ternes, T.A., 2015. Occurrence of venlafaxine, other antidepressants and selected metabolites in the Rhine catchment in the face of climate change. Environ. Pollut. 196, 247–256.

Schymanski, E.L., Jeon, J., Gulde, R., Fenner, K., Ruff, M., Singer, H.P., Hollender, J., 2014. Identifying small molecules via high resolution mass spectrometry: communicating confidence. Environ. Sci. Technol. 48 (4), 2097–2098.

Silva, L.J., Lino, C.M., Meisel, L.M., Pena, A., 2012. Selective serotonin re-uptake inhibitors (SSRIs) in the aquatic environment: an ecopharmacovigilance approach. Sci. Total Environ. 437, 185–195.

Silva, L.J., Pereira, A.M., Meisel, L.M., Lino, C.M., Pena, A., 2014. A one-year follow-up analysis of antidepressants in Portuguese wastewaters: occurrence and fate, seasonal influence, and risk assessment. Sci. Total Environ. 490, 279–287.

Silva, L.J., Pereira, A.M., Meisel, L.M., Lino, C.M., Pena, A., 2015. Reviewing the serotonin reuptake inhibitors (SSRIs) footprint in the aquatic biota: uptake, bioaccumulation and ecotoxicology. Environ. Pollut. 197, 127–143.

Suarez, S., Lema, J.M., Omil, F., 2010. Removal of pharmaceutical and personal care products (PPCPs) under nitrifying and denitrifying conditions. Water Res. 44 (10), 3214–3224.

Suarez, S., Reif, R., Lema, J.M., Omil, F., 2012. Mass balance of pharmaceutical and personal care products in a pilot-scale single-sludge system: influence of T, SRT and recirculation ratio. Chemosphere 89 (2), 164–171.

Subedi, B., Kannan, K., 2015. Occurrence and fate of select psychoactive pharmaceuticals and antihypertensives in two wastewater treatment plants in New York State, USA. Sci. Total Environ. 514, 273–280.

Thomaidi, V.S., Stasinakis, A.S., Borova, V.L., Thomaidis, N.S., 2015. Is there a risk for the aquatic environment due to the existence of the emerging organic contaminants in treated domestic wastewater? Greece as a case-study. J. Hazard. Mater 283, 740–747.

Vasskog, T., Berger, U., Samuelsen, P.J., Kallenborn, R., Jensen, E., 2006. Selective serotonin reuptake inhibitors in sewage influents and effluents from Tromso, Norway. J. Chromatogr. A 1115 (1–2), 187–195.

Vasskog, T., Anderssen, T., Pedersen-Bjergaard, S., Kallenborn, R., Jensen, E., 2008. Occurrence of selective serotonin reuptake inhibitors in sewage and receiving waters at Spitsbergen and in Norway. J. Chromatogr. A 1185 (2), 194–205.

Wick, A., Wagner, M., Ternes, T.A., 2011. Elucidation of the transformation pathway of the opium alkaloid codeine in biological wastewater treatment. Environ. Sci. Technol. 45 (8), 3374–3385.

Zanger, U.M., 2012. Introduction to drug metabolism. In: Anzenbacher, P., Zanger, U.M. (Eds.), Metabolism of Drugs and Other Xenobiotics. Wiley-VCH Verlag GmbH & Co. KGaA, Weinheim, Germany.

Zonja, B., Goncalves, C., Perez, S., Delgado, A., Petrovic, M., Alpendurada, M.F., Barcelo, D., 2014. Evaluation of the phototransformation of the antiviral zanamivir in surface waters through identification of transformation products. J. Hazard. Mater 265, 296–304.